BIOCHEMISTRY
including biophysical chemistry & molecular biology
Article

Biochemistry **2011,** *50,* 1857–1863 1857
DOI: 10.1021/bi1014997

Enhanced Base-Pair Opening in the Adenine Tract of a RNA Double Helix[†]

Yuegao Huang, Xiaoli Weng, and Irina M. Russu*

Department of Chemistry and Molecular Biophysics Program, Wesleyan University, Middletown, Connecticut 06459, United States

Received September 15, 2010; Revised Manuscript Received January 19, 2011

ABSTRACT: Proton exchange and nuclear magnetic resonance spectroscopy are being used to characterize the kinetics and energetics of base-pair opening in two nucleic acid double helices. One is the RNA duplex 5′-r(GCGAUAAAAAGGCC)-3′/5′-r(GGCCUUUUUAUCGC)-3′, which contains a central tract of five AU base pairs. The other is the homologous DNA duplex with a central tract of five AT base pairs. The rates and the equilibrium constants of the opening reaction of each base pair are measured from the dependence of the exchange rates of imino protons on ammonia concentration, at 10 °C. The results reveal that the tract of AU base pairs in the RNA duplex differs from the homologous tract of AT base pairs in DNA in several ways. The rates of opening of AU base pairs in RNA are high and increase progressively along the tract, reaching their largest values at the 3′-end of the tract. In contrast, the opening rates of AT base pairs in DNA are much lower than those of AU base pairs. Within the tract, the largest opening rate is observed for the AT base pair at the 5′-end of the tract. These differences in opening kinetics are paralleled by differences in the stabilities of individual base pairs. All AU base pairs in the RNA are less stable than the AT base pairs in the DNA. The presence of the tract enhances these differences by increasing the stability of AT base pairs in DNA while decreasing the stability of AU base pairs in RNA. Due to these divergent trends, along the tracts, the AU base pairs become progressively less stable than AT base pairs. These findings demonstrate that tracts of AU base pairs in RNA have specific dynamic and energetic signatures that distinguish them from similar tracts of AT base pairs in DNA.

Homopolymeric runs of adenines are overabundant in the genomes of eukaryotes (*1*). Their properties have been extensively characterized, revealing the important role played by the base sequence in the structure and dynamics of the DNA double helix (*2*, *3*). The structure of these adenine tracts is distinct from that of canonical B-form DNA: the helix has a shorter helical repeat, the base pairs are highly propeller-twisted, the minor groove becomes progressively narrower along the tract, and additional bonding between bases may occur through bifurcated hydrogen bonds across the major groove. At the global level, adenine tracts repeated in phase with the helical repeat induce the curvature of the double helix (*2*). The unusual structural features of adenine tracts also give rise to large variations in DNA dynamics. For example, NMR[1] measurements have shown that the AT base pairs in the interior of the tract open much less frequently than AT base pairs in generic DNA base sequences (*4*−*6*). These structural and dynamic features have been correlated to the mechanical properties of the tracts and to the participation of the tracts in chromatin organization (*3*).

Characterization of adenine tracts in other structural contexts has lagged behind that in DNA. Do adenine tracts in other structural contexts, such as RNA duplexes or RNA−DNA hybrids, maintain the unusual structural and dynamic properties observed in DNA? The full answer to this question is not yet known. Early optical melting experiments have shown that RNA and RNA−DNA hybrid duplexes containing tracts of adenines are significantly less stable than their homologous DNA counterparts (*7*). Similarly, our laboratory has recently found that the stability of individual dA-rU base pairs in the adenine tract of a RNA−DNA hybrid is greatly reduced relative to that of dA-dT base pairs in DNA. Moreover, the location of the base pair in the tract affects its stability differently in DNA and in the RNA−DNA hybrid (*8*).These results have suggested that the properties of adenine tracts depend on the structural context in which the tract is placed. To gain further insight into this dependence, in the present work, we have characterized the opening kinetics and the stability of individual base pairs in the RNA duplex shown in Figure 1. The RNA contains a tract of AU base pairs that extends from the 6th to the 10th position of the duplex. GC/CG base pairs are added at the ends to increase the stability of the duplex and to prevent the effects of fraying upon the AU base pairs of interest. The results for the RNA duplex are compared to those for the homologous DNA duplex that contains a tract of AT base pairs (Figure 1). The base sequence of the DNA duplex is present in the λ tR2 intrinsic transcription termination site, previously studied by our laboratory (*8*).

EXPERIMENTAL PROCEDURES

Materials. The DNA and RNA strands were synthesized using solid-support phosphoramidite chemistry on an automated DNA synthesizer. 3-^{15}N-labeled 2′-O-tom-protected uridine phosphoramidite was prepared as described previously (*8*) and was used for the synthesis of ^{15}N-labeled RNA strands. The DNA and RNA strands were purified by reverse-phase HPLC on

[†]This work was supported by a grant from the National Institutes of Health (GM077188).

*To whom correspondence should be addressed. Phone: (860) 685-2428. Fax: (860) 685-2211. E-mail: irussu@wesleyan.edu.

[1]Abbreviations: NMR, nuclear magnetic resonance; fHSQC, fast heteronuclear single-quantum coherence; NOESY, nuclear Overhauser effect spectroscopy.

Published on Web 01/20/2011

A.

RNA Duplex

```
      1   2   3   4   5   6   7   8   9   10  11  12  13  14
5′- r(G   C   G   A   U   A   A   A   A   A   G   G   C   C)  -3′
3′-  (C   G   C   U   A   U   U   U   U   U   C   C   G   G)r -5′
```

DNA Duplex

```
      1   2   3   4   5   6   7   8   9   10  11  12  13  14
5′- d(G   C   G   A   T   A   A   A   A   A   G   G   C   C)  -3′
3′-  (C   G   C   T   A   T   T   T   T   T   C   C   G   G)d -5′
```

B.

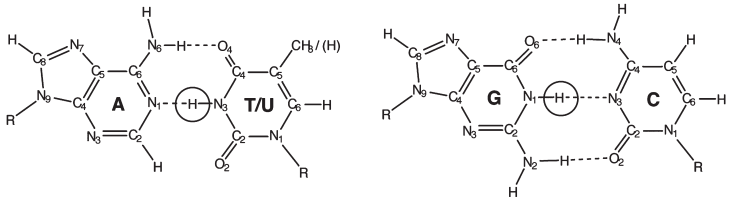

FIGURE 1: (A) Base sequences and numbering of base pairs in the two nucleic acid duplexes investigated. (B) Structures of AT/AU and GC base pairs with the imino protons highlighted.

a PRP-1 semipreparative column (Hamilton) in 50 mM triethylamine acetate buffer with a gradient of 5−32% acetonitrile in 46 min at 60 °C. The counterions were replaced with Na^+ ions by repeated centrifugation in Amicon Ultra-4 centrifugal filter units using 0.5 M NaCl, followed by repeated centrifugation against water.

The final NMR samples contained 0.1−0.8 mM duplexes in 10 mM phosphate buffer with 18 mM sodium ions and 0.5 mM EDTA in 90% H_2O/10% D_2O at pH 7.8 ± 0.1 (at 10 °C). The samples also contained 0.5 mM triethanolamine, which was used to measure the pH of the sample directly in the NMR tube as we have described (*9*).

Methods. NMR Experiments. The NMR experiments were performed at 10 °C on a Varian INOVA 500 spectrometer operating at 11.75 T. One-dimensional spectra were obtained with the jump-and-return pulse sequence (*10*) and, for ^{15}N-labeled samples, with the fast heteronuclear single-quantum coherence (fHSQC) pulse sequence (*11*) to edit the resonances of protons attached to ^{15}N. The $^1H-^1H$ NOESY spectra were obtained with the Watergate pulse sequence (*12*) with a mixing time of 250 ms.

The proton exchange rates were measured using the method of transfer of magnetization from water. In these experiments, the exchange was initiated by inverting selectively the water magnetization using a Gaussian 180° pulse (5.8 ms). A variable delay (τ) was allowed following water inversion for exchange to occur. A weak gradient (0.21 G/cm) was applied during this delay to prevent the effects of radiation damping upon the recovery of water magnetization to equilibrium. At the end of the exchange delay, a second Gaussian pulse (2 ms) was applied to bring the water magnetization back onto the *z*-axis. Twenty-five values of the exchange delay τ, in the range from 1 to 800 ms, were used in each experiment. For the unlabeled samples, the observation was with the jump-and-return pulse sequence. For the ^{15}N-labeled samples, the observation was with the fHSQC pulse sequence. The obtained exchange rates were independent of the pulse sequence used for observation. The highest exchange rates that can be measured reliably using these methods are ~70−90 s^{-1} at 10 °C.

The exchange rates were calculated from the dependence of the intensity of the imino proton resonance of interest on the exchange delay τ. This dependence is expressed by the equation (*13*):

$$I(\tau) = I^0 + [I(0) - I^0 - A]e^{-(R_1 + k_{ex})\tau} + Ae^{-R_{1w}\tau} \quad (1)$$

where I^0 is the intensity at equilibrium, $I(0)$ is the intensity immediately after the first selective pulse on water, k_{ex} is the exchange rate, and R_1 is the longitudinal relaxation rate of the observed proton. The factor A is defined as

$$A = \left[\frac{I_w(0)}{I_w^0} - 1\right]\left(\frac{k_{ex}}{R_1 + k_{ex} - R_{1w}}\right)I^0 \quad (2)$$

where $I_w(0)$ and I_w^0 are the intensities of the water proton resonance after the inversion pulse and at equilibrium, respectively, and R_{1w} is the longitudinal relaxation rate of water protons. $I_w(0)$, I_w^0, and R_{1w} were measured in separate experiments (*13*) at each ammonia concentration investigated. An example of the calculation of the exchange rates is provided in Supporting Information.

Imino Proton Exchange in Nucleic Acids. Our characterization of the two nucleic acid duplexes relies upon the exchange of imino protons (Figure 1) with solvent protons. This process occurs via a structural opening reaction that brings the imino proton into an open state. In this state, the hydrogen bond holding the imino proton is broken, and the imino proton is accessible to proton acceptors present in the solvent, for example, NH_3 (*14*). The exchange rate observed experimentally depends on the concentration of proton acceptor B as (*14*, *15*)

$$k_{ex} = \frac{k_{op}k_B[B]}{k_{cl} + k_B[B]} \quad (3)$$

where k_{op} and k_{cl} are the opening and the closing rate of the base pair containing the imino proton and k_B is the rate constant for the transfer of the imino proton to the acceptor B, in the open state of the base pair. The rates of opening and closing define the

equilibrium constant of the opening reaction:

$$K_{op} = \frac{k_{op}}{k_{cl}} \quad (4)$$

This equilibrium constant is related to the free energy change in the opening reaction by

$$\Delta G_{op} = -RT \ln K_{op} \quad (5)$$

where T is the absolute temperature and R is the universal gas constant.

Two kinetic regimes for imino proton exchange can be distinguished depending on the concentration of proton acceptor. In the EX1 regime, the concentration of proton acceptor is high such that $k_B[B] \gg k_{cl}$ and, as eq 3 shows, the exchange rate equals the rate of base-pair opening. At low proton acceptor concentrations (namely, $k_B[B] \ll k_{cl}$, EX2 regime), the exchange rate is simply proportional to the concentration of proton acceptor:

$$k_{ex} = K_{op} k_B [B] \quad (6)$$

In the present work we have used ammonia base (NH_3) as the acceptor in imino proton exchange. The rate constants for the transfer of imino protons to NH_3 at 10 °C are 4.1×10^8 M^{-1} s^{-1} for thymine and 8.8×10^8 M^{-1} s^{-1} for guanine and uracil (*16*). Increasing concentrations of ammonia base were obtained by titrating the sample with small volumes of a stock ammonia solution (0.5 or 3 M). The concentration of ammonia base was calculated from the total ammonia concentration C_0 and the pH as

$$[NH_3] = C_0 \left(\frac{10^{-pK}}{10^{-pH} + 10^{-pK}} \right) \quad (7)$$

The pH was measured at each ammonia concentration, directly in the NMR tube, using the proton resonances of triethanolamine (*9*). The pK value of ammonia at 10 °C is 9.73 (*17*).

RESULTS

The NMR resonances of the imino protons in the two nucleic acid duplexes investigated are shown in Figure 2. In the DNA duplex, the resonances were previously assigned by this laboratory (*8*).[2] The imino proton resonances of the RNA duplex were assigned using site-specific ^{15}N-editing and $^1H-^1H$ NOESY. The ^{15}N-editing experiments were carried out on six RNA duplexes in which a single uracil base, labeled with ^{15}N at the N3 position, was placed in each of the following positions: 4, 6, 7, 8, 9, and 10. The edited spectra (Figure 3) provide the position of the resonance of the labeled uracil in the spectrum as follows: AU_4 at 13.98 ppm, AU_6 at 12.88 ppm, AU_7 at 13.55 ppm, AU_8 at 13.61 ppm, AU_9 at 13.74 ppm, and AU_{10} at 13.90 ppm. The imino proton resonance of the remaining uracil (UA_5 at 13.22 ppm) is assigned from its NOESY connectivity to the resonance of AU_4 (Figure 4). Sequential NOESY connectivities are also observed for the other uracil imino proton resonances whose chemical shifts are sufficiently different from each other, for example, AU_6 (12.88 ppm) to AU_7 (13.55 ppm), AU_8 (13.61 ppm) to AU_9 (13.74 ppm), and AU_9 (13.74 ppm) to AU_{10} (13.90 ppm). The uracil imino protons also show the expected connectivities to adenine C2 protons (right panel in Figure 4). The imino proton resonances of GC_{11}, GC_{12}, and CG_{13} are assigned from sequential connectivities between imino protons (Figure 4), namely, AU_{10} (13.90 ppm) to GC_{11} (12.88 ppm), GC_{11} (12.88 ppm) to GC_{12} (13.32 ppm), and GC_{12} (13.32 ppm) to CG_{13} (13.47 ppm). The imino proton resonances of CG_2 and GC_3 are assigned from the connectivities of the imino proton to adenine C2 or guanine amino protons. The adenine C2 proton of AU_4 (7.58 ppm) shows a connectivity to the imino proton at 12.11 ppm, which assigns the latter resonance to GC_3. In turn, the amino proton of GC_3 at 8.25 ppm shows a connectivity to the imino proton of CG_2 at 12.88 ppm.

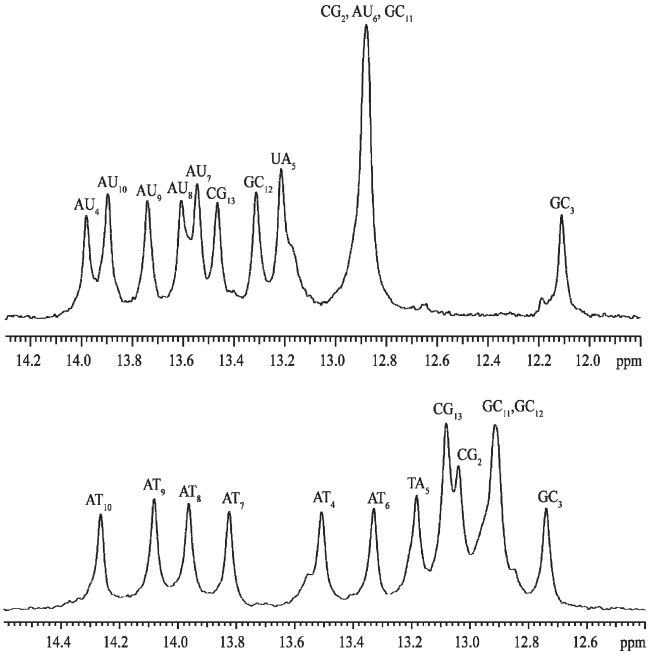

FIGURE 2: NMR resonances of imino protons in the RNA duplex (upper spectrum) and in the DNA duplex (lower spectrum) at pH 7.8 and at 10 °C. The resonances of the DNA duplex[2] were previously assigned by our laboratory (*8*). The assignments of the resonances of the RNA duplex are described in the text.

The rates of exchange of imino protons with solvent protons were measured as a function of the concentration of proton acceptor (NH_3). For the RNA duplex, the measurements were carried out on both unlabeled and ^{15}N-labeled samples (Figures 2 and 3). Representative examples of the results for the exchange of imino protons in AT and AU base pairs of the two duplexes are presented in Figure 5. The results for the remaining imino protons in AU and GC/CG base pairs are shown in Supporting Information. For most imino protons the dependence of the exchange rate on the proton acceptor concentration is that predicted by eq 3. The only exception is the AU_{10} base pair in the RNA duplex (Figure 5). In this case, the exchange rate increases sharply with increasing ammonia concentration and, when it becomes higher than ~70 s^{-1}, cannot be measured accurately by the NMR transfer of magnetization technique.

The imino proton exchange rates were fitted as a function of the concentration of proton acceptor to eq 3 (or to eq 6 for AU_{10}). The opening rate, k_{op}, and the closing rate, k_{cl}, for each base pair, obtained from these fits, are summarized in Table 1. The table includes also the values of the equilibrium constant, K_{op}, and the free energy change in the opening reaction, ΔG_{op}, for each base pair, which were calculated based on eqs 4 and 5, respectively.

[2]The numbering of base pairs in the DNA duplex differs from that used in our previous publication. Here, the base pairs are numbered in increasing order in the 5′ → 3′ direction on the DNA A-rich strand while, in our previous publication, the base pairs were numbered in increasing order in the 5′ → 3′ direction on the DNA T-rich strand.

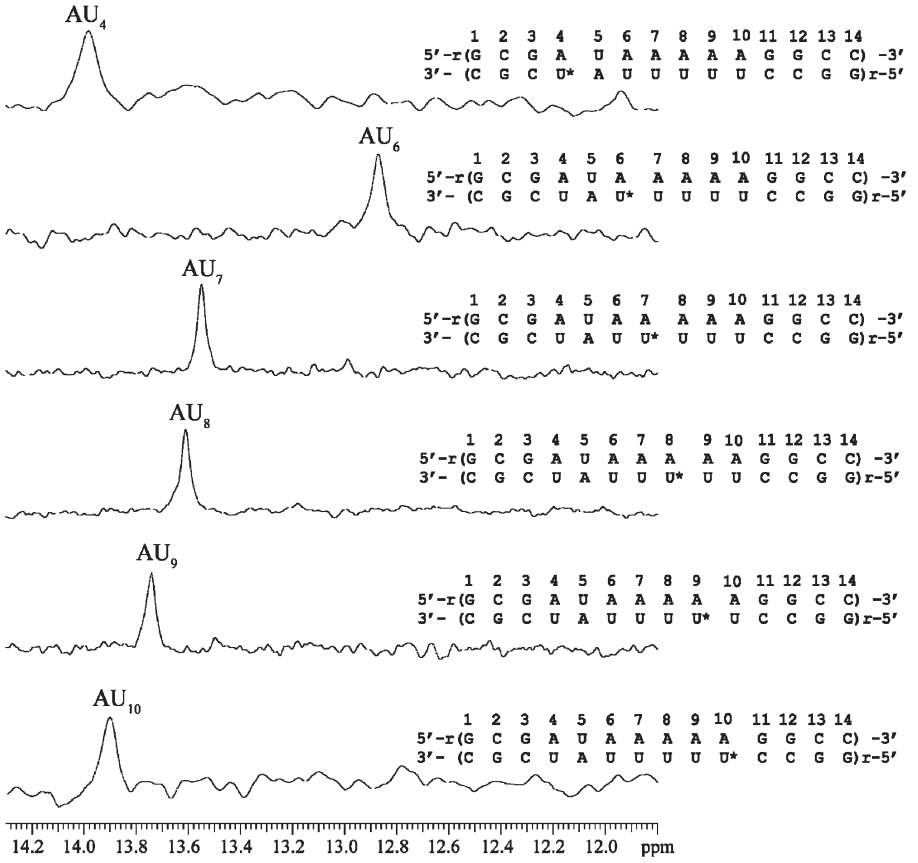

FIGURE 3: ^{15}N-edited NMR resonances of imino protons for six RNA duplex molecules in which a single uracil was labeled with ^{15}N. The ^{15}N-labeled uracil in each molecule is indicated by an asterisk.

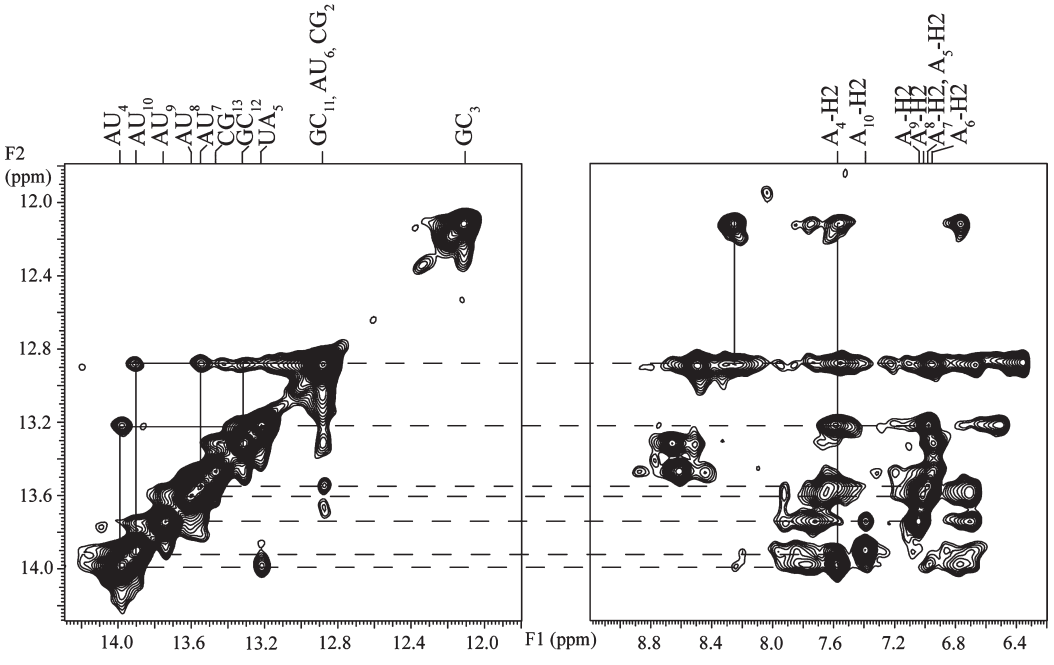

FIGURE 4: Selected regions of the ^{1}H−^{1}H NOESY spectrum of the RNA duplex showing connectivities between imino protons (left panel) and between imino and adenine C2/guanine amino protons (right panel).

DISCUSSION

Previous work from this and other laboratories has demonstrated that the base-pair opening in DNA tracts of AT base pairs has a unique pattern whose main features are as follows: (i) the opening rates of the base pairs inside these tracts are much lower than those of AT base pairs in random sequence contexts, and (ii) for the first AT base pair in the tract (i.e., the base pair formed by the adenine at the 5′-end of an A_n or an A_nT_n tract), the opening rate is comparable to or higher than opening rates of AT base pairs in random sequence contexts (*4*, *6*, *18*, *19*). These

dynamic properties have been correlated to the structure of AT tracts (*4*), to the ability of the tracts to bend the DNA double helix (*4*), and to the role of the tracts in the organization of nucleosomes (*3*).

Our present results on the DNA duplex confirm these previous observations (Table 1). For the base pairs situated in the interior of the tract (i.e., AT_7, AT_8, and AT_9), the opening rates are $\sim$3 s^{-1}. This value is $\sim$4-fold lower than the opening rates of the base pairs that are not part of the tract, TA_5 and AT_4 ($k_{op} \approx 11$ s^{-1}). For the first base pair in the tract, AT_6, the opening rate (17 s^{-1}) is higher than the rates of all other AT base pairs, within and outside the tract. This profile for the opening of AT base pairs in the DNA duplex is illustrated in Figure 6.

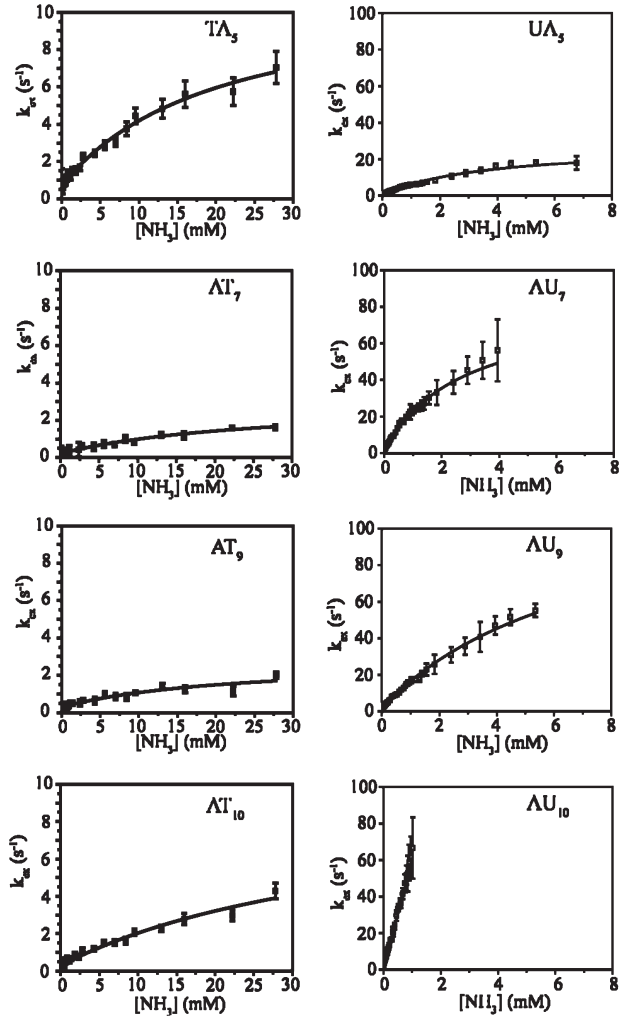

FIGURE 5: Dependence of the imino proton exchange rates on the concentration of ammonia base for selected AT/TA base pairs in the DNA duplex (left panels) and the corresponding AU/UA base pairs in the RNA duplex (right panels). The scale for the exchange rates in the RNA duplex is 10 times larger than that in the DNA duplex. The curves represent nonlinear least-squares fits to eq 3. The line for AU_{10} in the RNA duplex is a fit to eq 6.

The opening kinetics of AU base pairs in the RNA duplex is very different from that of AT base pairs in the DNA duplex. The opening rates for most AU base pairs are higher than those of AT base pairs: $\sim$3-fold higher for base pairs in the fourth and fifth positions, $\sim$30-fold higher for base pairs in the seventh and eighth positions, and $\sim$45-fold higher for the base pair in the ninth position (Table 1). These changes profoundly affect the dynamic profile of the AU tract in the RNA duplex (Figure 6). In the first position of the tract, the opening rate of the AU base pair in the RNA is comparable to that of the AT base pair in the DNA. The largest differences are seen in the interior of the tract: in the DNA, the opening rates are low and relatively constant throughout the tract, while in the RNA, the rates are higher and increase gradually as one advances inside the tract. The opening rates of AU base pairs inside the tract are also 3−4-fold higher than those of AU base pairs outside the tract (AU_4 and UA_5). These results therefore demonstrate that the tract of AU base pairs in the RNA duplex has its own dynamic signature that is clearly distinguishable from that of the AT tract in DNA.

The opening rates of AU base pairs in RNA duplexes of various base sequences have been previously measured by Leroy and co-workers (*20*). In agreement with our present results, these authors found that, in random sequence contexts, the rates of opening of AU base pairs in RNA duplexes are increased relative

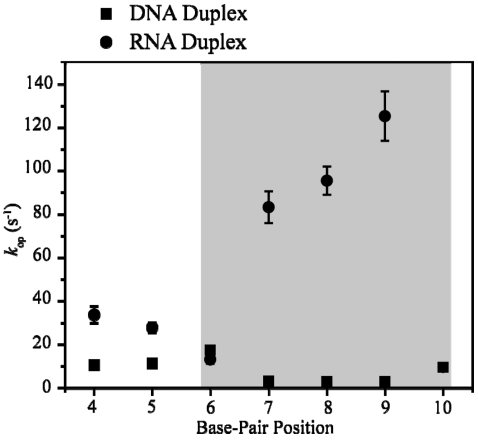

FIGURE 6: Opening rates of AT/TA and AU/UA base pairs in the two duplexes investigated. The experimental errors for the values in the DNA duplex are smaller than the symbols. The shaded area highlights the location of the tracts of AT or AU base pairs.

Table 1: Opening Parameters for AU and AT Base Pairs in the Nucleic Acid Duplexes Investigated at 10 °C

RNA duplex					DNA duplex				
base pair	k_{op} (s^{-1})	k_{cl} ($\times 10^{-7}$ s^{-1})	K_{op} ($\times 10^6$)	ΔG_{op} (kcal/mol)	base pair	k_{op} (s^{-1})	k_{cl} ($\times 10^{-7}$ s^{-1})	K_{op}[b] ($\times 10^6$)	ΔG_{op}[b] (kcal/mol)
AU_4	34 ± 4	0.42 ± 0.06	8 ± 1	6.6 ± 0.1	AT_4	10.6 ± 0.7	0.54 ± 0.08	1.9 ± 0.3	7.40 ± 0.09
UA_5	28 ± 2	0.33 ± 0.04	8 ± 1	6.58 ± 0.08	TA_5	11.3 ± 0.7	0.8 ± 0.1	1.4 ± 0.2	7.60 ± 0.08
AU_6	13 ± 2	0.06 ± 0.02	22 ± 8	6.0 ± 0.2	AT_6	17 ± 2	1.7 ± 0.3	1.0 ± 0.2	7.7 ± 0.1
AU_7	83 ± 7	0.25 ± 0.03	33 ± 5	5.79 ± 0.08	AT_7	3.0 ± 0.5	1.1 ± 0.3	0.28 ± 0.09	8.5 ± 0.2
AU_8	95 ± 6	0.29 ± 0.02	32 ± 3	5.81 ± 0.06	AT_8	3 ± 1	2 ± 2	0.1 ± 0.1	8.9 ± 0.5
AU_9	125 ± 11	0.65 ± 0.07	19 ± 3	6.10 ± 0.08	AT_9	2.8 ± 0.6	0.9 ± 0.4	0.3 ± 0.1	8.4 ± 0.3
AU_{10}	−[a]	−[a]	63 ± 1	5.44 ± 0.01	AT_{10}	9 ± 2	1.7 ± 0.5	0.5 ± 0.2	8.1 ± 0.2

[a]The exchange rates in the EX1 regime are too fast to be measured by NMR (Figure 5). [b]From ref *8*.

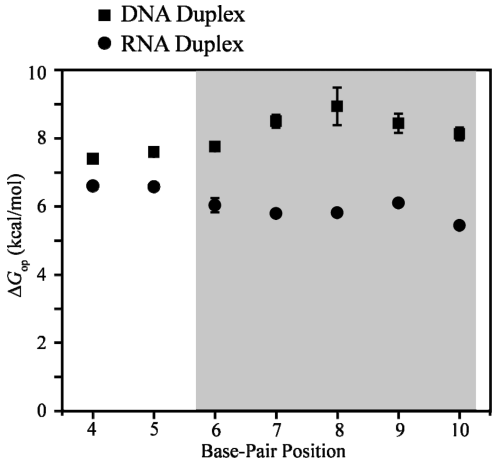

FIGURE 7: Opening free energy changes for AT/TA and AU/UA base pairs in the two duplexes investigated. The shaded area highlights the location of the tracts of AT or AU base pairs.

to those of AT base pairs in homologous DNA duplexes. One RNA duplex investigated in this study contained a tract of eight AU base pairs: (5′-rGGUUUUUUUUCC-3′/5′-GGAAAAAA-AACC-3′). The base-pair opening profile for the tract was not obtained, however, because the imino proton resonances of seven of the AU base pairs overlapped. Instead, an apparent opening rate was calculated from the exchange rate of the overlapped resonance, and was found to be 2−10-fold higher than the opening rates of AT base pairs in DNA duplexes.

In addition to opening rates, the results obtained in our work also allow the stability of each AU base pair in the RNA to be compared to that of the corresponding AT base pair in the DNA. In our approach, the stability of an individual base pair is evaluated from the equilibrium constant of the opening reaction (K_{op}, eq 4) or from the opening free energy change (ΔG_{op}, eq 5). Stable base pairs are characterized by small K_{op} and large ΔG_{op} values. An increase in K_{op}, and the accompanying decrease in ΔG_{op}, reflects a destabilization of the base pair.

The free energy changes for opening of AU base pairs in the RNA duplex are compared to those for AT base pairs in the DNA duplex in Figure 7. For the positions outside the tract, the AU base pairs are slightly less stable than the AT pairs (i.e., the ΔG_{op} values in the RNA duplex are smaller than those in the DNA duplex by 0.8−1 kcal/mol, Table 1). Inside the tract, the differences in stability between AT and AU base pairs in homologous positions are enhanced. In the DNA duplex, the ΔG_{op} values are higher than those outside the tract, indicating an increase in base-pair stability. In contrast, in the RNA duplex, the ΔG_{op} values decrease relative to those outside the tract. Due to these divergent trends, as one advances within the tracts, the AU base pairs become progressively less stable than the AT base pairs. The largest difference is attained at the central eighth position where the AU base pair is ~3 kcal/mol less stable than the AT base pair. It is interesting to note also that the lower stabilities of AU base pairs in the RNA result from changes in both base-pair opening and base-pair closing reactions (eq 4). For example, for the AU_7 base pair in the RNA the opening equilibrium constant, K_{op}, is ~120-fold higher than that of the AT_7 base pair in the DNA (Table 1). This increase is due to an ~30-fold increase in the opening rate, k_{op}, and to an ~4-fold decrease in the closing rate, k_{cl}. Similar changes are observed for all the other AU base pairs, with the exception of the first base pair in the tract. As discussed above, the opening rate of AU_6 in the RNA is comparable to that of AT_6 in the DNA (Table 1). Yet, the closing rate of AU_6 is ~30-fold lower than that of AT_6. The closing rate is related to the lifetime of the base pair in the open state (τ_{op}) by

$$k_{cl} = \frac{1}{\tau_{op}} \quad (8)$$

Hence, the lower stability of the first AU base pair in the RNA tract is solely due to an increase in the lifetime of the base pair in the open, extrahelical state.

The differences in dynamics and stability of individual base pairs that we observed between RNA tracts of AU base pairs and DNA tracts of AT pairs must originate from specific structural features of these tracts, which affect base-pair opening reactions. Molecular dynamics simulations have characterized base-pair opening transitions in atomic detail (*21*−*23*). During opening, the base unstacks from neighboring bases and swings out of the helix through either the major or the minor groove. In the resulting extrahelical state, all hydrogen bonds, in which the base participates in the native structure, are broken. Several structural features of AT tracts in DNA can affect their opening. First, the high propeller twists of AT base pairs enhance the stacking interactions between adenine bases in one strand and between thymine bases in the other strand (*24*−*26*). Second, the narrow minor groove allows formation of a spine of hydration that bridges the thymine of one strand to the adenine of the opposite strand (*25*, *27*). Third, according to some crystallographic structures, bifurcated hydrogen bonds can form across the major groove, between the adenine in one strand and the adjacent thymine in the other strand (*24*−*26*, *28*). These structural characteristics of AT tracts are expected to lower opening rates and enhance base-pair stability, in agreement with our results for the DNA duplex.

The structural basis for the higher opening rates and the lower stability of tracts of AU base pairs in RNA is not yet fully understood. This is due, at least in part, to the paucity of structures that have been solved for these tracts in RNA. One factor that contributes to the lower stability of AU base pairs, relative to AT base pairs, is the absence of the C5 methyl group in uracil. The C5 methyl group of thymine improves the base-stacking energy of adjacent AT base pairs at A-A and A-T steps, as previously demonstrated by other laboratories (*29*, *30*). An additional explanation is provided by the recent NMR structure of a 44-nucleotide RNA responsible for dynein-mediated localization of the *Drosophila fs*(*1*) *K10* transcript. This RNA was found to fold into a stem−loop structure (*31*). One of the helices in the stem contains a tract of five AU base pairs and assumes the A′-form conformation (*32*, *33*). In this conformation, the major groove is wider and more accessible than in the canonical A-form. Furthermore, the base stacking is very different from that in canonical A- and B-forms: there is continuous stacking of the adenine bases on one strand, while the stacking of uracil bases on the other strand is greatly reduced. The latter feature should enhance the opening dynamics and lower the intrahelical stability of the uracil bases, as we observe here for the RNA duplex.

In summary, in the present work, we have shown that tracts of AU base pairs in RNA possess dynamic and energetic features that distinguish them from homologous AT tracts in DNA. The opening of AU base pairs within the tracts is faster and energetically less costly than that of AT base pairs. The kinetics of opening also exhibits a strong dependence on the position of

the base pair in the tract, with the AU base pairs at the 3′-end of the tract being the most labile. These properties provide dynamic and energetic signals that may be used in the folding of RNA sequences containing AU tracts and in the binding of ligands to these tracts.

ACKNOWLEDGMENT

We thank Dr. Michael Calter (Wesleyan University) for help with the synthesis of 3-^{15}N-labeled 2′-O-tom-protected uridine phosphoramidite.

SUPPORTING INFORMATION AVAILABLE

Figures showing the results of transfer of magnetization experiments and the dependence of imino proton exchange rates on ammonia base concentration for selected AU and GC/CG base pairs in the two nucleic acid duplexes investigated. This material is available free of charge via the Internet at http://pubs.acs.org.

REFERENCES

1. Dechering, K. J., Cuelenaere, K., Konings, R. N. H., and Leunissen, J. A. M. (1998) Distinct frequency-distributions of homopolymeric DNA tracts in different genomes. *Nucleic Acids Res. 26*, 4056–4062.
2. Haran, T. E., and Mohanty, U. (2009) The unique structure of A-tracts and intrinsic DNA bending. *Q. Rev. Biophys. 42*, 41–81.
3. Segal, E., and Widom, J. (2009) Poly(dA:dT) tracts: major determinants of nucleosome organization. *Curr. Opin. Struct. Biol. 19*, 65–71.
4. Leroy, J. L., Charretier, E., Kochoyan, M., and Gueron, M. (1988) Evidence from base-pair kinetics for two types of adenine tract structures in solution: their relation to DNA curvature. *Biochemistry 27*, 8894–8898.
5. Moe, J. G., and Russu, I. M. (1990) Proton exchange and base pair opening kinetics in 5′-d(CGCGAATTCGCG)-3′ and related dodecamers. *Nucleic Acids Res. 18*, 821–827.
6. Moe, J. G., Folta-Stogniew, E., and Russu, I. M. (1995) Energetics of base-pair opening in a DNA dodecamer containing an A_3T_3 tract. *Nucleic Acids Res. 23*, 1984–1989.
7. Martin, F. H., and Tinoco, I. J. (1980) RNA-DNA hybrid duplexes containing oligo (dA:rU) sequences are exceptionally unstable and may facilitate termination of transcription. *Nucleic Acids Res. 8*, 2295–2299.
8. Huang, Y., Weng, X., and Russu, I. M. (2010) Structural energetics of the adenine tract from an intrinsic transcription terminator. *J. Mol. Biol. 397*, 677–688.
9. Chen, C., and Russu, I. M. (2004) Sequence-dependence of the energetics of opening of AT base pairs in DNA. *Biophys. J. 87*, 1–7.
10. Plateau, P., and Gueron, M. (1982) Exchangeable proton NMR without base-line distortion, using new strong-pulse sequences. *J. Am. Chem. Soc. 104*, 7310–7311.
11. Mori, S., Abeygunawardana, C., Johnson, M. O., and van Zijl, P. C. M. (1995) Improved sensitivity of HSQC spectra of exchanging protons at short interscan delays using a new fast HSQC(FHSQC) detection scheme that avoids water saturation. *J. Magn. Reson. B 108*, 94–98.
12. Lippens, G., Dhalluin, C., and Wieruszeski, J.-M. (1995) Use of a water flip-back pulse in the homonuclear NOESY experiment. *J. Biomol. NMR 5*, 327–331.
13. Russu, I. M. (2004) Probing site-specific energetics in proteins and nucleic acids by hydrogen exchange and NMR spectroscopy. *Methods Enzymol. 379*, 152–175.
14. Englander, S. W., and Kallenbach, N. R. (1984) Hydrogen exchange and structural dynamics of proteins and nucleic acids. *Q. Rev. Biophys. 16*, 521–655.
15. Gueron, M., and Leroy, J.-L. (1995) Studies of base pair kinetics by NMR measurement of proton exchange. *Methods Enzymol. 261*, 383–413.
16. Huang, Y., Chen, C., and Russu, I. M. (2009) Dynamics and stability of individual base pairs in two homologous RNA-DNA hybrids. *Biochemistry 48*, 3988–3997.
17. Weast, R. C. (1987) CRC Handbook of Chemistry and Physics, 67th ed., CRC Press, Boca Raton, FL.
18. Moe, J. G., and Russu, I. M. (1992) Kinetics and energetics of base-pair opening in 5′-d(CGCGAATTCGCG)-3′ and a substituted dodecamer containing G·T mismatches. *Biochemistry 31*, 8421–8428.
19. Warmlander, S., Sen, A., and Leijon, M. (2000) Imino proton exchange in DNA catalyzed by ammonia and trimethylamine: evidence for a secondary long-lived open state of the base pair. *Biochemistry 39*, 607–615.
20. Snoussi, K., and Leroy, J.-L. (2001) Imino proton exchange and base-pair kinetics in RNA duplexes. *Biochemistry 40*, 8898–8904.
21. Varnai, P., and Lavery, R. (2002) Base flipping in DNA: pathways and energetics studied with molecular dynamics simulations. *J. Am. Chem. Soc. 124*, 7272–7273.
22. Giudice, E., Varnai, P., and Lavery, R. (2003) Base pair opening within B-DNA: free energy pathways for GC and AT base pairs from umbrella sampling simulations. *Nucleic Acids Res. 31*, 1434–1443.
23. Priyakumar, U. D., and MacKerell, A. D., Jr. (2006) Computational approaches for investigating base flipping in oligonucleotides. *Chem. Rev. 106*, 489–505.
24. Nelson, H. C. M., Finch, J. T., Luisi, B. F., and Klug, A. (1987) The structure of an oligo(dA)·oligo(dT) tract and its biological implications. *Nature 330*, 221–226.
25. DiGabriele, A. D., and Steitz, T. A. (1993) A DNA dodecamer containing an adenine tract crystallizes in a unique lattice and exhibits a new bend. *J. Mol. Biol. 231*, 1024–1039.
26. MacDonald, D., K., H., Zhang, X., Polgruto, T., and Lu, P. (2001) Solution structure of an A-tract DNA bend. *J. Mol. Biol. 306*, 1081–1098.
27. Woods, K. K., Maehigashi, T., Howerton, S. B., Sines, C. C., Tannenbaum, S., and Williams, L. D. (2004) High-resolution structure of an extended A-tract: $[d(CGCAAATTTGCG)]_2$. *J. Am. Chem. Soc. 126*, 15330–15331.
28. Coll, M., Frederick, C. A., Wang, A. H.-J., and Rich, A. (1987) A bifurcated hydrogen-bonded conformation in the d(A·T) base pairs of the DNA dodecamer d(CGCAAATTTGCG) and its complex with distamycin. *Proc. Natl. Acad. Sci. U.S.A. 84*, 8385–8389.
29. Wang, S., and Kool, E. T. (1995) Origins of the large differences in stability of DNA and RNA helices: C-5 methyl and 2′-hydroxyl effects. *Biochemistry 34*, 4125–4132.
30. Warmlander, S., Sponer, J. E., Sponer, J., and Leijon, M. (2002) The influence of the thymine C5 methyl group on spontaneous base pair breathing in DNA. *J. Biol. Chem. 277*, 28491–28497.
31. Bullock, S. L., Ringel, I., Ish-Horowicz, D., and Lukavsky, P. J. (2010) A′-form RNA helices are required for cytoplasmic mRNA transport in Drosophila. *Nat. Struct. Mol. Biol. 17*, 703–710.
32. Arnott, S., Hukins, D. W., and Dover, S. D. (1972) Optimised parameters for RNA double-helices. *Biochem. Biophys. Res. Commun. 48*, 1392–1399.
33. Saenger, W. (1983) Principles of Nucleic Acid Structure, Springer-Verlag, New York.